Prediction of Molecular Weight Distributions by Probability Generating Functions. Application to Industrial Autoclave Reactors for High Pressure Polymerization of Ethylene and Ethylene-Vinyl Acetate

A. BRANDOLIN *and* C. SARMORIA*

Planta Piloto de Ingeniería Química (PLAPIQUI)-UNS-CONICET
Camino La Carrindanga km 7-8000 Bahía Blanca, Argentina

A. LÓPEZ-RODRÍGUEZ, K. S. WHITELEY, *and* B. DEL AMO FERNÁNDEZ

Dirección I+D (Repsol-YPF)-C/Embajadores 183
28045 Madrid, Spain

We develop a mathematical model able to describe the complete molecular weight distributions of polyethylene and ethylene-vinyl acetate copolymers obtained in high pressure autoclave reactors. We apply probability generating function definitions to the mass balances of radical and polymer species in the reacting medium. We use three different definitions of probability generating functions, each one directly applicable either to the number, weight or chromatographic distributions. These probability generating functions are numerically inverted to obtain the corresponding calculated molecular weight distribution. The capabilities of two different inversion methods are compared. Predictions are compared with experimental data obtained in an industrial reactor; good agreement is obtained. The approach presented here is applicable to other types of polymerization reactors and post-polymerization processes.

INTRODUCTION

Polyolefins and their derivatives are among the most widely used polymers. Their versatility is partly due to the possibility of producing many different grades of material by changing reactor design or operating conditions. This work deals with the high pressure production of LDPE and EVA copolymers in autoclave reactors. In these polymers final properties depend directly on average molecular weight, molecular weight distribution and short and long chain branching indexes. In turn, those characteristics may be changed by manipulating several operating conditions in the autoclave reactors, such as reactor temperature, pressure, initiator and chain-transfer agent concentrations. It is therefore important to be able to simulate, and better yet to predict, the relevant polymer properties given the design and operating conditions of a polymerization reactor. Advancing in the theoretical modeling of the process would help to improve our understanding of the influence of reactor design and operating conditions on the structure of polymer molecules, and finally aid in the design of new products, as well as optimization strategies prior to production at commercial scale.

In this work we present a mathematical model of the polymerization process in autoclave reactors that may calculate the complete molecular weight distribution of the product given its reactor design and operating conditions. We focus on reactors that follow the ICI process configuration, with several sections connected in series. Operating pressures range from 0.98 $\times 10^8$ to 1.96 $\times 10^8$ Pa, while temperatures are set at different levels covering the range from 150 to 300°C from the first to the last section. Conversions of about 20% are typical in these reactors.

In a previous work (1) we reported a moment model coupled with a mixing model (2) developed in Repsol-YPF for its autoclave reactors. This combined model is capable of predicting temperatures, concentrations,

*Corresponding author. E-mail: csarmoria@plapiqui.edu.ar

average molecular weights, long chain branching indexes and melt flow indexes for polyethylene and EVA at any point in the present type of reactors. The input to that model consists of concentrations of monomer, initiators, transfer agent, global polymer and radicals, plus several values related to the design of the reactor. Model parameter adjustment was performed using experimental information from Repsol-YPF's reactors. After this process it was possible to adequately match calculated and experimental average molecular weights of polymers obtained under a wide range of operating conditions (1).

In the present work we build on the previous moment-mixing model to be able to predict the complete molecular weight distribution of the polymers obtained in these reactors. To this purpose we establish a simplified set of mass balances for the reactor species that does not include the usual quasi-steady state approximation, and apply a transform technique. The chosen transform is the probability generating function (pgf). Three different pgfs were defined, to describe the number, weight and chromatographic distributions, respectively. Pgfs are calculated along the reactor. They are numerically inverted using the inversion methods and procedures analyzed in Brandolin *et al.* (3). This allows recovery of the molecular weight distributions. The moments of the distributions are needed as input, so they are calculated with the previous moment-mixing model with the kinetic values previously reported (1).

Other transforms could be applied to the mass balance equations (4, 5) as is well described in Brandolin *et al.* (3). The pgf transforms considered in this work are defined for discrete distributions, as those found in polymer science, and their transformed variable is real and bounded. This makes them attractive to be used in a simulation involving polymeric species, such as the one in this work.

It must be noted that the inversion step is the most difficult stage in any transformation method. In most cases the inversion must be accomplished numerically, so error propagation commonly produces oscillations in the recovered molecular weight distribution. Since it is impossible to distinguish numerical noise from actual peaks in the distribution, this poses a serious problem. We use here the inversion procedures employed in Brandolin *et al.* (3), which are promising in this respect.

With respect to molecular weight distribution prediction in LDPE reactors, a few different approaches have been proposed in the past. For autoclave reactors, Lorenzini *et al.* (6) start from mass balances on classical chemical species such as initiator or monomer, and on pseudo components such as the moments of the MWD. Once the moments have been calculated, they are used to estimate the MWD as a deformation of the log-normal distribution. In a similar way, Brandolin *et al.* (7) calculate four moments of the distribution from mass balances in a tubular reactor, and use them to estimate the MWD as a skewed log normal distribution. This requires estimation of four parameters, something achieved in their work through a nonlinear regression to minimize the difference between the moments of the analytic distribution and those obtained from the moment balances. Nordhus *et al.* (8) use a kinetic model and recursive expressions to calculate both MWD and long-chain branching distributions for LDPE obtained in high pressure reactors. The reactors are divided into several interconnected volumes, which are modeled as CSTRs. One of the examples they present is a calculation on a reactor that closely resembles an industrial equipment using 31 such volumes. The authors convert their originally discrete model into a continuous differential-integral-algebraic model in order to take advantage of computational tools available for convolution integrations in continuous functions. They compare their calculated long-chain branching distributions for several resin grades with "experimental" values calculated from intrinsic viscosity measurements. No comparison with experimental data was performed for the corresponding MWD. Pladis and Kiparissides (9) also evaluate a joint distribution of molecular weight and long chain branching content for LDPE obtained in autoclave reactors. Unlike Nordhus *et al.* (8), they divide the population of molecules into classes according to their number of branches. Moment balances are performed for each class, and the calculated moments are used to estimate the two parameters of an assumed log normal distribution. The total distribution is then found by a weighted sum of the class distributions. Pladis and Kiparissides (9) reviewed other general works on models for polymerization in autoclave reactors. None of them attempts the use of probability generating functions.

On the other hand, Whiteley and Garriga (10) obtained reasonable MWD curves when inverting generating functions at definite values of a transformed variable. These generating functions were those reported by Jackson *et al.* (4) for a theoretical radical polymerization in continuous stirred tank reactors.

PGF MODEL

Figure 1 shows a scheme of a typical section of an autoclave reactor for LDPE and EVA production, divided into cells according to a previous mixing model (2). Probability generating function definitions for the number, weight and chromatographic chain distributions of radicals and polymer must be applied to the corresponding mass balances at each one of the cells in which the studied reactor is divided. In what follows we present the kinetic mechanism, the mass and moment balances, and finally the detailed description of the application of the probability generating functions to this problem.

Kinetic Mechanism

The proposed reaction mechanism is basically the same previously reported (1). The long-chain branches are not considered here because our primary interest is the molecular weight distribution.

The following basic reactions (*Eqs 1–7*), considered to be important in the polymerization of ethylene alone or in presence of vinyl acetate, are included in the model:

Peroxide Initiation

$$I_j \xrightarrow{f_j k_{cj}} 2\ R(0) \quad j = 1 \ldots NIT \tag{1}$$

Propagation

$$R(x) + M \xrightarrow{k_p} R(x+1) \tag{2}$$

Termination by Combination

$$R(x) + R(y) \xrightarrow{k_{tc}} P(x+y) \tag{3}$$

Thermal Degradation (scission)

$$R(x) \xrightarrow{k_{tdt}} P(x) + R(0) \tag{4}$$

Chain Transfer to Polymer

$$R(x) + P(y) \xrightarrow{y\,k_{trp}} P(x) + R(y) \tag{5}$$

Chain Transfer to Solvent

$$R(x) + S_j \xrightarrow{k_{trsj}} P(x) + R(0) \quad j = 1 \ldots NST \tag{6}$$

Chain Transfer to Monomer

$$R(x) + VA \xrightarrow{k_{trm}} P(x) + R(1) \tag{7}$$

The kinetic constant for the transfer to polymer reaction is given per monomeric unit in the polymer, since the rate of this reaction is proportional to the polymer length. That is why the length of the polymer, y, appears with the rate constant in *Eq 5*. For an explanation of the symbols used, please refer to the **Nomenclature** section at the end of the paper.

We assume that this mechanism is adequate to describe both ethylene homopolymerization and ethylene-vinyl acetate copolymerization. We treat the monomer mixture as a pseudo monomer identified as "M", as described in a previous work (1). The values for the kinetic rate constants were the same used in that previous work.

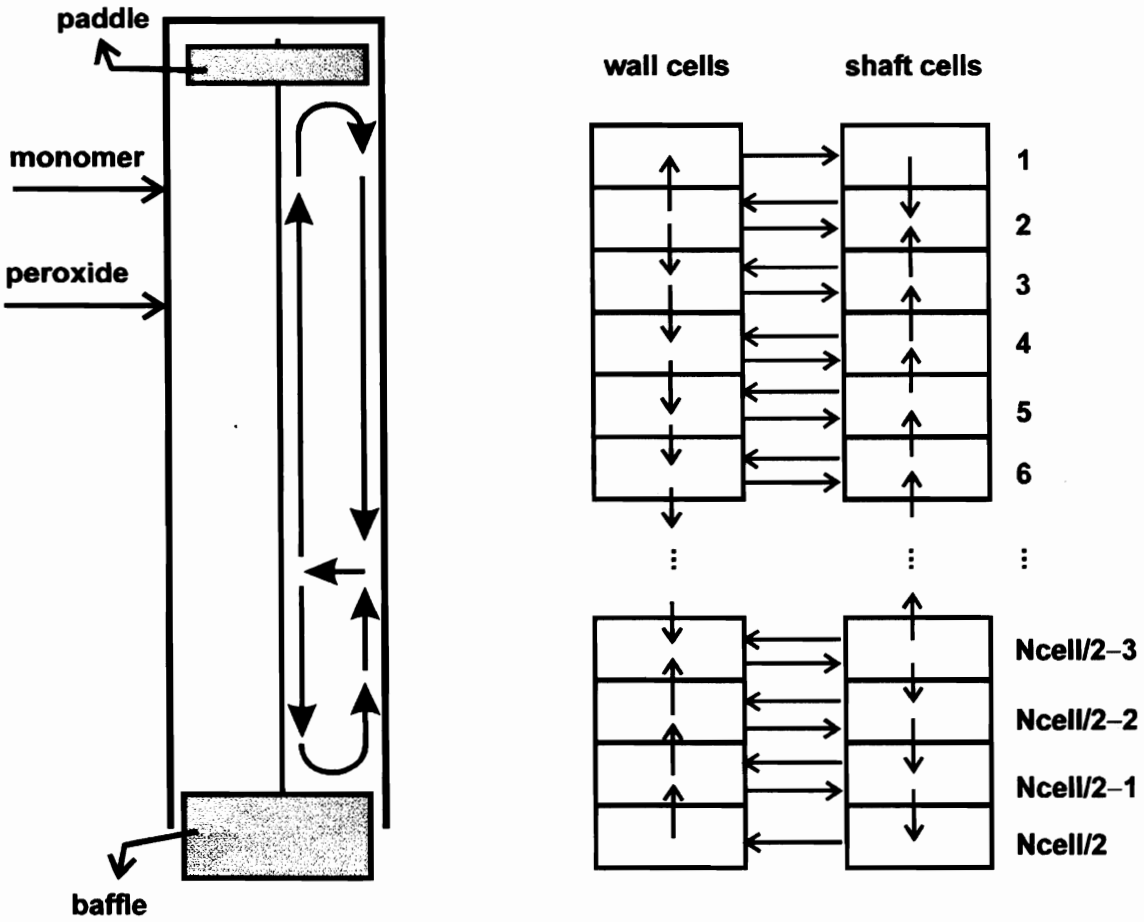

Fig. 1. Scheme of a generic zone of the autoclave reactor and its flow pattern.

Mass Balances

The stationary mass balances for all the species present at each one of the cells in which the reactor is divided are shown in *Eqs 8–10.*

Global Monomer at Cell "k" (k = ks or kw, ks = 1, 2... Ncell/2, kw = 1, 2,...Ncell/2)

$$0 = \sum_{i=1}^{Nin_k} [M]_{in_i} F_{Vin_i} - \sum_{i=1}^{Nout_k} [M]_k F_{V\,out_i} - k_{p_k}[M]_k \sum_{y=0}^{\infty} [R(y)]_k V_k - k_{trm_k}[VA]\left(\sum_{y=0}^{\infty} [R(y)]_k - [R(0)]_k\right)V_k \tag{8}$$

Radicals $R(x)$ $(x = 0, 1, 2,...\infty)$ at *Cell "k"* (*k = ks* or *kw, ks = 1, 2,...Ncell/2, kw = 1, 2,...Ncell/2*)

$$0 = \sum_{i=1}^{Nin_k} [R(x)]_{in_i} F_{Vin_i} - \sum_{i=1}^{Nout_k} [R(x)]_k F_{Vout_i} + \sum_{i=1}^{NIT} 2f_j k_{cj_k} [I_j]_k \delta_{x0} V_k - k_{p_k}[M]_k [R(x)]_k V_k + k_{p_k}[M]_k [R(x-1)]_k V_k - 2k_{tc_k}[R(x)]_k \sum_{y=0}^{\infty} [R(y)]_k V_k - k_{tdt_k}[R(x)]_k (1-\delta_{x0}) V_k + k_{tdt_k}\left(\sum_{y=0}^{\infty} [R(y)]_k - [R(0)]_k\right)\delta_{x0} V_k - k_{trp_k}[R(x)]_k (1-\delta_{x0}) \sum_{y=1}^{\infty} y[P(y)]_k V_k + k_{trp_k}\left(\sum_{y=0}^{\infty} [R(y)]_k - [R(0)]_k\right) x[P(x)]_k V_k - \sum_{j=1}^{NST} k_{trs_{j_k}}[R(x)]_k(1-\delta_{x0})[S_j]_k V_k + \sum_{j=1}^{NST} k_{trs_{j_k}} \left(\sum_{y=0}^{\infty} [R(y)]_k - [R(0)]_k\right)[S_j]_k \delta_{x0} V_k - k_{trm_k}[R(x)]_k (1-\delta_{x0}) [VA]V_k + k_{trm_k}\left(\sum_{y=0}^{\infty} [R(y)]_k - [R(0)]_k\right)\delta_{x1}[VA]V_k \tag{9}$$

Polymer P(x) (x = 1, 2,...∞) at cell "k" (k = ks or kw, ks = 1, 2,...Ncell/2, kw = 1, 2,...Ncell/2)

$$0 = \sum_{i=1}^{Nin_k} [P(x)]_{in_i} F_{Vin_i} - \sum_{i=1}^{Nout_k} [P(x)]_k F_{Vout_i} + k_{tc_k} \sum_{y=0}^{x} [R(y)]_k [R(x-y)]_k V_k + k_{tdt_k}[R(x)]_k V_k + k_{trp_k}[R(x)]_k \sum_{y=1}^{\infty} y[P(y)]_k V_k - k_{trp_k}\left(\sum_{y=0}^{\infty} [R(y)]_k - [R(0)]_k\right) xP(x)_k V_k + \sum_{j=1}^{NST} k_{trs_{j_k}}[R(x)]_k [S_j]_k V_k + k_{trm_k}[R(x)]_k [VA]V_k \tag{10}$$

As the radical and polymer molecules may have any length between 0 and infinity, the mass balance equations are infinite in number. Special techniques are necessary to overcome this difficulty. The ones chosen for this work are explained below.

Moment Balances

When the objective is to obtain average molecular weights, the above infinitely large set of equations may be bounded. This is accomplished by applying the moment technique, using the following moment definitions shown in *Eqs 11* and *12*:

nth Radical Moment

$$\lambda_n = \sum_{x=0}^{\infty} x^n [R(x)] \tag{11}$$

nth Polymer Moment

$$\mu_n = \sum_{x=1}^{\infty} x^n [P(x)] \tag{12}$$

To obtain the moment balance equations for radicals, both sides of *Eq 9* must be multiplied by $\sum_{x=0}^{\infty} x^n$. Similarly, to obtain the moment balance equations for the polymer, both sides of *Eq 10* must be multiplied by $\sum_{x=1}^{\infty} x^n$. Following this procedure, *Eqs 13* and *14* result.

Radical moment λ_n (n = 0, 1, 2) at cell "k" (k = ks or kw, ks = 1, 2,...Ncell/2, kw = 1, 2,...Ncell/2)

$$0 = \sum_{i=1}^{Nin_k} \lambda_{n\,in_i} F_{Vin_i} - \sum_{i=1}^{Nout_k} \lambda_{n_k} F_{Vout_i} + \sum_{j=1}^{NIT} 2f_j k_{cj_k} [I_j]_k \delta_{n0} V_k - k_{p_k}[M]_k \lambda_{n_k} V_k + k_{p_k}[M]_k \sum_{j=0}^{n} \binom{n}{j} \lambda_{j_k} V_k - 2k_{tc_k} \lambda_{n_k} \lambda_{0_k} V_k - k_{tdt_k}(\lambda_{n_k} - [R(0)]_k)V_k + k_{tdt_k}(\lambda_{0_k} - [R(0)]_k)\delta_{n0} V_k - k_{trp_k}(\lambda_{n_k} - [R(0)]_k) \mu_1 V_k + k_{trp_k}(\lambda_{0_k} - [R(0)]_k)\mu_{n+1_k} V_k - \sum_{j=1}^{NST} k_{trs_{j_k}} (\lambda_{n_k} - [R(0)]_k)[S_j]_k V_k + \sum_{j=1}^{NST} k_{trs_{j_k}}(\lambda_{0_k} - [R(0)]_k) [S_j]_k \delta_{n0} V_k - k_{trm_k}(\lambda_{m_k} - [R(0)]_k)[VA]\, V_k + k_{trm_k}(\lambda_{0_k} - [R(0)]_k)[VA]V_k \tag{13}$$

Polymer moment μ_n (n = 0, 1, 2) at cell "k" (k = ks or kw, ks = 1, 2,...Ncell/2, kw = 1, 2,...Ncell/2)

$$0 = \sum_{i=1}^{Nin_k} \mu_{n\,in_i} F_{Vin_i} - \sum_{i=1}^{Nin_k} \mu_{n_k} F_{Vin_i} + k_{tc_k} \sum_{i=0}^{n} \binom{n}{i} \lambda_{i_k} \lambda_{n-i_k} V_k + k_{tdt_k}(\lambda_{n_k} - [R(0)]_k)V_k + k_{trp_k}(\lambda_{n_k} - [R(0)]_k)\mu_{1_k} V_k - k_{trp_k}(\lambda_{0_k} - [R(0)]_k)\mu_{n+1_k} V_k + \sum_{j=1}^{NST} k_{trs_{j_k}} (\lambda_{n_k} - [R(0)]_k)[S_j]_k V_k + k_{trm_k}(\lambda_{n_k} - [R(0)]_k)[VA]V_k \tag{14}$$

It should be noted that μ_{n+1} appears in the balance of μ_n. When solving up to the second moment, *Eq 15* is used to estimate the polymer 3rd moment (1):

$$\mu_3 = \left(\frac{\mu_2}{\mu_1}\right)^2 \sqrt{2\mu_2\mu_0 - (\mu_1)^2}, \quad (15)$$

As we explain later, only the 0th, 1st and 2nd moments are necessary for the pgf calculations.

Basic Definitions on Probability Generating Functions

When calculating the complete MWD, we apply the concept of probability generating function (pgf) to the mass balance equations. Through proper inversion of the resulting pgf it is possible to obtain information of the entire molecular weight distribution.

The radical and polymer length distributions are described in three different forms in this work: in number, weight and chromatography basis. In a number distribution, all molecules have an equal chance of being randomly chosen. In a weight distribution, all units of mass are equally likely to be chosen. In a chromatographic distribution, the quantity to look for is the product of mass times the molecular weight. Those three distributions have associated probabilities. The probability that a certain fraction of radical molecules has a length "x" is symbolized by $P_j(X = x)$, $j = n, w$ or c. Now, given a discrete distribution of probabilities $P_j(X = x)$, the probability generating function is defined as shown in *Eq 16* (11):

$$\text{Radicals } \phi_{X,j}(z) = \sum_{x=0}^{\infty} P_j(X = x)z^x \quad j = n, w, c \quad (16)$$

If the probability distributions for polymers are symbolized by $P^*_j(X = x)$, we can also define pgfs for polymers, as indicated in *Eq 17*:

$$\text{Polymer } \psi_{X,j}(z) = \sum_{x=0}^{\infty} P_j^*(X = x)z^x \quad j = n, w, c \quad (17)$$

The transformed variable is "z", $0 \le z \le 1$. The pgf is a real, continuous, increasing, bounded function of z that may take values between 0 and 1. In order to define the various pgfs, it is necessary to calculate several different probabilities. The number distributions, $P_n(X = x)$ and $P^*_n(X = x)$, are calculated in *Eqs 18* and *19*:

$$\text{Radicals } P_n(X = x) = \frac{R(x)}{\sum_{x=0}^{\infty} R(x)} = \frac{R(x)}{\lambda_0} \quad (18)$$

$$\text{Polymer } P_n^*(X = x) = \frac{P(x)}{\sum_{x=0}^{\infty} P(x)} = \frac{P(x)}{\mu_0} \quad (19)$$

where $R(x)$ and $P(x)$ are the molar concentrations of radicals and polymer of length "x", respectively. The weight distributions are calculated using *Eqs 20* and *21*:

$$\text{Radicals } P_w(X = x) = \frac{x\,R(x)}{\sum_{x=0}^{\infty} x\,R(x)} = \frac{x\,R(x)}{\lambda_1} \quad (20)$$

$$\text{Polymer } P_w^*(X = x) = \frac{x\,P(x)}{\sum_{x=0}^{\infty} xP(x)} = \frac{x\,P(x)}{\mu_1} \quad (21)$$

Finally, if the focus is on the pgf of the chromatographic distribution (pgfc), the corresponding probabilities are given by *Eqs 22* and *23*.

$$\text{Radicals } P_c(X = x) = \frac{x^2\,R(x)}{\sum_{x=0}^{\infty} x^2\,R(x)} = \frac{x^2\,R(x)}{\lambda_2} \quad (22)$$

$$\text{Polymer } P_c^*(X = x) = \frac{x^2\,P(x)}{\sum_{x=0}^{\infty} x^2P(x)} = \frac{x^2\,P(x)}{\mu_2} \quad (23)$$

Other relationships used to derive the different pgf balances in the reactor are given by *Eqs 24* and *25* (12):

$$\phi_{X+1,j}(z) = z\phi_{X,j}(z) \quad \psi_{X+1,j}(z) = z\,\psi_{X,j}(z) \quad (24)$$

$$\phi'_{X,j}(z) = \sum_{x=1}^{\infty} xP_j(X = x)z^{x-1}$$

$$\psi'_{X,j}(z) = \sum_{x=1}^{\infty} xP_j^*(X = x)z^{x-1} \quad (25)$$

pgfn Balances

To obtain the pgfn balance equations for the number distribution of radicals and polymer, both sides of the mass balance *Eqs 9* and *10* must be multiplied by $\sum_{x=0}^{\infty} z^x$. It should be noted that $R(x) = P_n(X = x)\,\lambda_0$ and $P(x) = P_n^*(X = x)\,\mu_0$.

As an example of the methodology followed we present *Eq 26* with the derivation of the transfer to polymer term in the radical balance:

$$-k_{trp_k}\sum_{x=0}^{\infty} z^x[R(x)]_k(1 - \delta_{x,0})\sum_{y=0}^{\infty} y[P(y)]_k V_k + k_{trp_k}$$

$$\left(\sum_{y=0}^{\infty}[R(y)]_k - [R(0)]_k\right)\sum_{x=0}^{\infty} z^x\,x[P(x)]_k\,V_k = -k_{trp_k}$$

$$(\lambda_{0_k}\phi_{X,n}(z)_k - [R(0)]_k)\mu_{1_k}\,V_k +$$

$$k_{trp_k}\,z\psi'_{X,n}(z)_k\,\mu_{0_k}(\lambda_{0_k} - [R(0)]_k)V_k \quad (26)$$

Other terms are obtained in an analogous way. Once all terms are expressed as functions of the moment and pgf definitions, *Eqs 27* and *28* result.

Balance of pgfn for the radical number-distribution at cell "k" (k = ks or kw, ks = 1, 2,...Ncell/2, kw = 1, 2,...Ncell/2)

$$0 = \sum_{i=1}^{Nin_k} \lambda_{0_{in_i}} \phi_{X,n}(z)_{in_i} F_{Vin_i} - \sum_{i=1}^{Nout_k} \lambda_{0_k} \phi_{X,n}(z)_k F_{Vout_i} + \sum_{j=1}^{NIT} 2 f_j k_{c_{j_k}} [I_j]_k V_k + k_{p_k}[M]_k \lambda_{0_k}(z-1)\phi_{X,n}(z)_k V_k - 2k_{tc_k}\phi_{X,n}(z)_k (\lambda_{0_k})^2 V_k + k_{tdt_k}\lambda_{0_k}(-\phi_{X,n}(z)_k + 1) V_k - k_{trp_k}(\lambda_{0_k}\phi_{X,n}(z)_k - [R(0)]_k)\mu_{0_k} V_k + k_{trp_k} z\psi'_{X,n}(z)_k \mu_{0_k}(\lambda_{0_k} - [R(0)]_k)V_k - \sum_{j=1}^{NST} k_{trs_{jk}}\lambda_{0_k}(\phi_{X,n}(z)_k - 1)[S_j]_k V_k - k_{trm_k}(\lambda_{0_k}\phi_{X,n}(z)_k - R(0)_k)[M]_k + z k_{trm_k}\lambda_{0_k}[M]_k \quad (27)$$

Balance of pgfn for the polymer number-distribution at cell "k" (k = ks or kw, ks = 1, 2,...Ncell/2, kw = 1, 2,...Ncell/2)

$$0 = \sum_{i=1}^{Nin_k} \mu_{0in_i}\psi_{X,n}(z)_{in_i} F_{Vin_i} - \sum_{i=1}^{Nout_k} \mu_{0_k}\psi_{X,n}(z)_k F_{Vout_i} + k_{tc_k}(\lambda_{0_k})^2(\phi_{X,n}(z)_k)^2 V_k + k_{tdt_k}(\lambda_{0_k}\phi_{X,n}(z)_k - [R(0)]_k) V_k + k_{trp_k}(\lambda_{0_k}\phi_{X,n}(z)_k - [R(0)]_k)\mu_{1_k} V_k - k_{trp_k} z\psi'_{X,n}(z)_k \mu_{0_k}(\lambda_{0_k} - [R(0)]_k)V_k + \sum_{j=1}^{NST} k_{trs_{jk}}(\lambda_{0_k}\phi_{X,n}(z)_k - [R(0)]_k)[S_j]_k V_k + k_{trm_k}(\lambda_{0_k}\phi_{X,n}(z)_k - [R(0)]_k)[M]_k V_k \quad (28)$$

Three options may be followed from this point on. The first one is to obtain pgfw and pgfc from the relations between the different types of pgf. For example see *Eqs 29* and *30*.

$$\phi_{X,w}(z) = z\frac{\phi'_{X,n}(z)}{\phi'_{X,n}(1)} \quad (29)$$

$$\phi_{X,c}(z) = z\frac{\phi'_{X,w}(z)}{\phi'_{X,w}(1)} \quad (30)$$

The second option is to numerically invert the pgfn and obtain the number molecular weight distribution, and build the weight and chromatographic distributions from that one. The last approach consists of solving the corresponding equations for the weight and chromatographic pgfs and inverting them to obtain the corresponding molecular weight distributions. As has already been shown (3), this last approach is the best one, because it minimizes error propagation.

To obtain the pgfw balance equations for the weight distribution of radicals and polymer, both sides of *Eqs 9* and *10* must be multiplied by $\sum_{x=0}^{\infty} xz^x$. The following relationships must be considered: $xR(x) = P_w(X = x)\lambda_1$, $xP(x) = P^*_w(X = x)\mu_1$.

As an example, derivation of transfer to polymer terms in the radical balance is presented below (*Eq 31*):

$$- k_{trp_k}\sum_{x=0}^{\infty} xz^x[R(x)]_k(1-\delta_{x0})\sum_{y=0}^{\infty} y[P_j(y)]_k V_k + k_{trp_k}\left(\sum_{y=0}^{\infty}[R(y)]_k - [R(0)]_k\right)\sum_{x=0}^{\infty} z^x x^2[P(x)]_k V_k = - k_{trp_k}\lambda_{1_k}\phi_{X,w}(z)_k \mu_{1_k} V_k + k_{trp_k} z\psi'_{X,w}(z)_k \mu_{1_k}\lambda_{0_k} V_k \quad (31)$$

Other terms are derived similarly, until they become expressed as functions of $\phi_{X,n}(z)$, $\phi_{X,w}(z)$, $\psi_{X,n}(z)$, $\psi_{X,w}(z)$. Finally, *Eqs 32* and *33* result after rearranging terms.

Balance of pgfw for the radical weight- distribution at cell "k" (k = ks or kw, ks = 1, 2,...Ncell/2, kw = 1, 2,...Ncell/2)

$$0 = \sum_{i=1}^{Nin_k} \lambda_{1_{in_i}}\phi_{X,w}(z)_{in_i} F_{Vin_i} - \sum_{i=1}^{Nout_k} \lambda_{1_k}\phi_{X,w}(z)_k F_{Vout_i} + k_{p_k}[M]_k \lambda \quad \phi_{X,w_k}(z)_k (z-1) V_k + k_{p_k}[M]_k z\lambda_{0_k}\phi_{X,n}(z)_k V_k - k_{tdt_k}\lambda_{1_k}\phi_{X,w}(z)_k V_k - k_{trp_k}\lambda_{1_k}\phi_{X,w}(z)_k \mu_{1_k} V_k + k_{trp_k} z\psi'_{X,w}(z)_k \mu_{1_k}\lambda_{0_k} V_k - \sum_{j=1}^{NST} k_{trs_{j_k}}\lambda_{1_k}\phi_{X,w}(z)_k [S_j]_k V_k - k_{trm_k}\lambda_{1_k}\phi_{X,w}(z)_k[VA] V_k + k_{trm_k}\left(\sum_{y=0}^{\infty}[R(y)]_k - [R(0)]_k\right)[VA] z V_k \quad (32)$$

Balance of pgfw for the polymer weight-distribution at cell "k" (k = ks or kw, ks = 1, 2,...Ncell/2, kw = 1, 2,...Ncell/2)

$$0 = \sum_{i=1}^{Nin_k} \mu_{1in_i}\psi_{X,w}(z)_{in_i} F_{Vin_i} - \sum_{i=1}^{Nout_k} \mu_{1_k}\psi_{X,w}(z)_k F_{Vout_i} + 2k_{tc_k}\lambda_{1_k}\lambda_{0_k}\phi_{X,w}(z)_k\phi_{X,n}(z)_k V_k + k_{tdt_k}\lambda_{1_k}\phi_{X,w}(z)_k V_k + k_{trp_k}\lambda_{1_k}\phi_{X,w}(z)_k \mu_{1_k} V_k - k_{trp_k} z\psi'_{X,w}(z)_k \mu_{1_k}\lambda_{0_k} V_k + \sum_{j=1}^{NST} k_{trs_{j_k}}\lambda_{1_k}\phi_{X,w}(z)_k [S_j]_k V_k + k_{trm_k}\lambda_{1_k}\phi_{X,w}(z)_k[VA] V_k \quad (33)$$

To obtain the pgfc balances *Eqs 9* and *10* must be multiplied by $\sum_{x=0}^{\infty} x^2 z^x$. It should be considered that $x^2R(x) = P_c(X = x)\lambda_2$, $x^2P(x) = P^*_c(X = x)\mu_2$.

As an example, derivation of the transfer to polymer term for radicals is presented in *Eq 34*.

$$- k_{trp_k}\sum_{x=0}^{\infty} x^2 z^x[R(x)]_k(1-\delta_{x0})\sum_{y=0}^{\infty} y[P_j(y)]_k V_k + k_{trp_k}\left(\sum_{y=0}^{\infty}[R(y)]_k - [R(0)]_k\right)\sum_{x=0}^{\infty} z^x x^3[P(x)]_k V_k = - k_{trp_k}\lambda_{2_k}\phi_{X,c}(z)_k \mu_{1_k} V_k + k_{trp_k} z\psi'_{X,c}(z)_k \mu_{2_k}\lambda_{0_k} V_k \quad (34)$$

After working in all the terms and rearranging them as functions of $\phi_{X,n}(z)$, $\phi_{X,w}(z)$, $\phi_{X,c}(z)$, $\psi_{X,n}(z)$, $\psi_{X,w}(z)$, and $\psi_{X,c}(z)$, *Eqs 35* and *36* result:

Balance of pgfc for the radical chromatographic-distribution at cell "k" (k = ks or kw, ks = 1, 2,...Ncell/2, kw = 1, 2,...Ncell/2)

$$0 = \sum_{i=1}^{Nin_k} \lambda_{2in_i} \phi_{X,c}(z)_{in_i} F_{Vin_i} - \sum_{i=1}^{Nout_k} \lambda_{2_k} \phi_{X,c}(z)_k F_{Vout_i} +$$

$$k_{p_k}[M]_k \lambda_{2_k} \phi_{X,c}(z)_k (z-1) V_k + k_{p_k}[M]_k z$$

$$(2\lambda_{1_k} \phi_{X,w}(z)_k + \lambda_{0_k} \phi_{X,n}(z)_k) V_k - 2k_{tc_k} \phi_{X,c}(z)_k$$

$$\lambda_{0_k} \lambda_{2_k} V_k - k_{tdt_k} \lambda_{2_k} \phi_{X,c}(z)_k V_k - k_{trp_k}$$

$$\lambda_{2_k} \phi_{X,c}(z)_k \mu_{1_k} V_k + k_{trp_k} z \psi'_{X,c}(z)_k \mu_{2_k} \lambda_{0_k} V_k$$

$$- \sum_{j=1}^{NST} k_{trs_{j_k}} \lambda_{2_k} \phi_{X,c}(z)_k [S_j]_k V_k - k_{trm_k} \lambda_{2_k}$$

$$\phi_{X,c}(z)_k [VA] V_k + k_{trm_k} (\lambda_{0_k} - [R(0)]_k)[VA] z V_k \quad (35)$$

Balance of pgfc for the polymer chromatographic-distribution at cell "k" (k = ks or kw, ks = 1, 2,...Ncell/2, kw = 1, 2,...Ncell/2)

$$0 = \sum_{i=1}^{Nin_k} \mu_{2in_i} \psi_{X,c}(z)_{in_i} F_{Vin_i} - \sum_{i=1}^{Nout_k} \mu_{k} \psi_{X,c}(z)_k F_{Vout_i} +$$

$$2k_{tc_k}\left(\lambda_{0_k} \lambda_{2_k} \phi_{X,n}(z)_k \phi_{X,c}(z)_k V_k + (\lambda_{1_k})^2 (\phi_{X,w}(z)_k)^2 V_k\right)$$

$$+ k_{tdt_k} \lambda_{2_k} \phi_{X,c}(z)_k V_k + k_{trp_k} \lambda_{2_k} \phi_{X,c}(z)_k \mu_{1_k} V_k$$

$$- k_{trp_k} z \psi'_{X,c}(z)_k \mu_{2_k} \lambda_{0_k} V_k + \sum_{j=1}^{NST} k_{trs_{j_k}} \lambda_{2_k} \phi_{X,c}(z)_k$$

$$[S_j]_k V_k + k_{trm_k} \lambda_{2_k} \phi_{X,c}(z)_k [VA] V_k \quad (36)$$

Pgf Model Resolution

First the simplified mixing-moment model (*Eqs 8* and *13–15*) is solved as explained in Sarmoria *et al.* (1). Initiator, solvent and monomer concentrations; temperature, internal fluxes, radical and polymer moments (λ_0, λ_1, λ_2, μ_0, μ_1, μ_2) at each cell are provided as results by the simplified mixing-moment model.

To obtain the stationary values for pgfn, pgfw and pgfc for radicals and polymers at each cell and obviously at the reactor exit, *Eqs 27*, *28*, *32*, *33*, *35*, and *36* must be solved at each of the selected values of the transformed variable z, $0 \le z \le 1$.

The selected z values must be at least the ones required by the numeric inversion algorithm to be used, in our case Gaver's and Stehfest's algorithms (3), which will be described in the next section. Other z values may be incorporated in the calculations in order to improve the accuracy in the numerical estimation of pgf first derivatives, which appear in all the pgf equations for the polymer. These derivatives were calculated by finite differences.

If an efficient nonlinear equation solver and adequate memory storage in the computer are available, all equations for the up to 514 z values may be solved simultaneously. Otherwise, equations for smaller sets of z values may be solved sequentially. Please note that pgf equations must be solved at least for two z values simultaneously, because of the terms where the pgf derivatives appear. We follow the latter approach to keep the size of the problem small enough to be handled by an ordinary personal computer. The values of $\phi_{X,j}$ and $\psi_{X,j}$ (j = n,w,c) must be calculated for ordered values of the transformed variable z, in order to be able to calculate the pgf derivatives with respect to z. Calculations may start either at $z = 1$ or at $z = 0$, since the values of both $\phi_{x,j}$ and $\psi_{x,j}$ are known at those particular points. We found better results, with smaller numerical noise, when starting at $z = 0$ and using backward differences for the evaluation of derivatives. That starting point was used for all the calculations reported in this work.

The different reactor sections are solved sequentially, all cells of the section at the same time because they are connected through internal flows. Arbitrary initial values between 0 and 1 are assumed for the pgf at each reactor cell, for each one of the z. We solve the system of nonlinear equations using a modified Powell hybrid algorithm (13) with a finite difference Jacobian.

Since each section in the reactor may be divided into around 50 cells, a large system of equations results. Specifically, the number of equations to be solved at each reactor section is given by *Eq 37*:

$$N_{eq} = 12\, Ncell\, N_z \quad (37)$$

The output of the pgf model consists of pgfn, pgfw and pgfc at each reactor cell and of course at the reactor exit. These quantities serve as data for the inversion algorithms (3). When inverting pgfn, the number molecular weight distribution is obtained directly. Inversion of pgfw and pgfc results in weight and chromatographic molecular weight distributions, respectively. Emphasis is placed on the MWD at the exit of the reactor, since this is the only point where experimental information is available for comparison.

PGF INVERSION ALGORITHMS

We use in this work the inversion formulas proposed by Gaver (14) and by Stehfest (15, 16) as adapted for the inversion of pgf transforms. Details may be found in Brandolin *et al.* (3).

Equation 38 shows Gaver's formula

$$f(\log(M_i)) \approx P_h(n) = \frac{2^h P_{h-1}(n) - P_{h-1}(n/2)}{2^h - 1},\ n = 2^h \quad (38)$$

where M_i is the molecular weight of fraction i, h is the extrapolation parameter, and $P_h(n)$ is recursively calculated by means of *Eq 39*.

$$P_0(n) = \frac{(2n)!}{n!\,(n-1)!}\,\frac{\ln(2)}{\log(M_i)}\sum_{k=0}^{n}\left(\binom{n}{k}(-1)^k\, pgf[z_k]\right) \tag{39}$$

where pgf[z_k] is the probability generating function calculated at $z_k = e^{-(n+k)\ln(2)/\log(M_i)}$.

Equations 40 and *41* show Stehfest's extrapolation formulas, where the method parameter is N.

$$f(\log(M_i)) \approx \ln(2)/t\sum_{n=1}^{N} K_n\, pgf(e^{-n\ln(2)/\log(M_i)}) \tag{40}$$

$$K_n = (-1)^{n+N/2}\sum_{k=[(n+1)/2]}^{\min(n,\,N/2)} \frac{k^{N/2}\,(2k)!}{(N/2-k)!k!(k-1)!(n-k)!(2k-n)!} \tag{41}$$

Each method has an optimum parameter value (h or N) that may vary with the particular problem studied. This optimum value was selected according to the SSQ1 criterion (3). This criterion indicates that the optimum value of the parameter is the one that minimizes the sum of squares of the differences between curves calculated with two successive values of N or h.

The computational effort required by each method may be estimated by the number of times (N_T) the pgf must be calculated for a given number of molecular weight points (N_w). *Equations 42* and *43* give N_T for Gaver's and Stehfest's methods, respectively, as function of the method parameter:

$$N_{T,\,G} = N_w\, 2^{h+1} \tag{42}$$

$$N_{T,\,S} = N_w N \tag{43}$$

EXPERIMENTAL VALIDATION

The reactor features and operating range have already been reported (1). Two polyethylenes (PE-1 and PE-2) and two copolymers (EVA-7, EVA-17) were selected to check our model results. The properties of these polymers are representative of the range of molecular properties produced in the studied reactors. Molecular weight distributions (MWD) of product samples were obtained by Size Exclusion Chromatography (SEC) in a Waters 150C equipment, using TCB as solvent and 0.04 wt% of Irganox 1010 as stabilizer at 145°C. The operating conditions were as follows: flow rate 0.7 mL/min, sample concentration 5 mg/mL and injection volume 150 μL. The resulting measured molecular weight distributions are shown in the Results section.

As a first step we calculated the pgfn, pgfw, and pgfc from the measured MWD, in order to compare them with the ones calculated by pgf balances. We followed the same procedure as in Brandolin *et al.* (3) to convert the experimental data into pgfs.

We show in *Fig. 2* the curves for pgfn, pgfw and pgfc corresponding to the polymer at the exit of the reactor

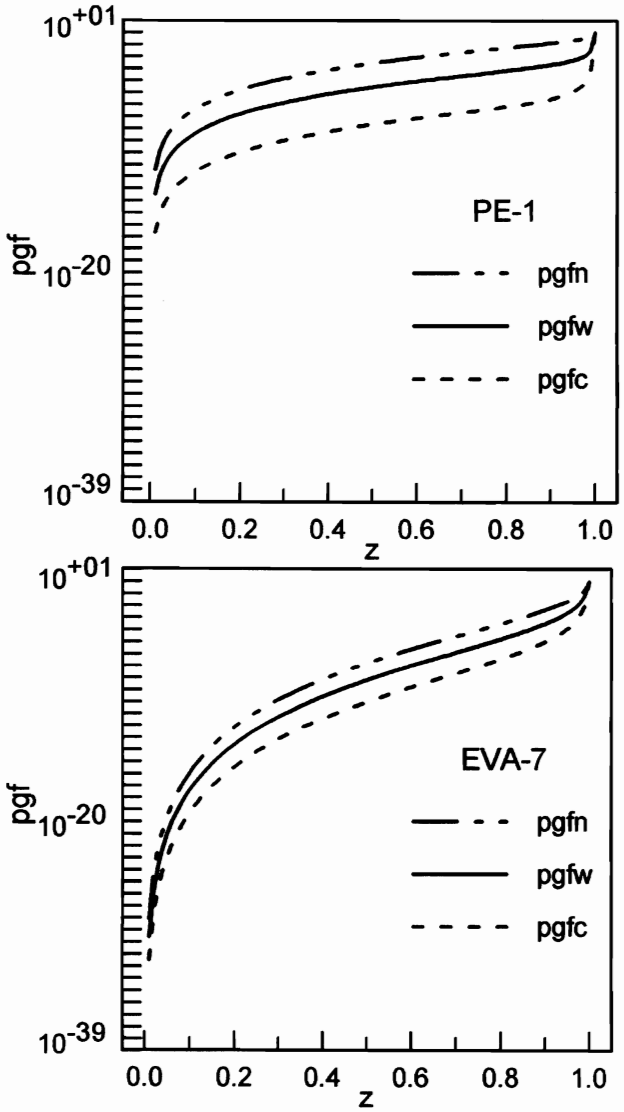

Fig. 2. Probability generating functions calculated from experimental MWDs.

for two of the selected experimental cases. In all cases it was observed that the order pgfn ≥ pgfw ≥ pgfc is always preserved. As expected, all the pgfs are continuous increasing functions of z. In spite of the similitude between the pgfs of the various polymers, the curves differ in magnitude and slope. This accounts for the capability of pgfs of saving information on the complete MWD. Moreover, the different average molecular weights of the polymers are reflected in the different slopes of the pgfs at z = 1 (11).

RESULTS AND DISCUSSION

We discuss first the pgf model results for one of the fully detailed examples already presented as PE-B in our previous publication (1). It corresponds to a simulation of a two-section reactor where ethylene is polymerized. A baffle divides the reactor into a 274 m^3 top

Table 1. Operating Conditions and Simulation Results for PE-B Example Simulation.

Section	T_{set} (°C)	P (Pa)	Fg (kg/h)	S (Mw = 42) (% w/w)	Initiator (mol/h)	$Conv_{out}$ (%)	Mn_{out}	Mw_{out}	Mz_{out}	Ln_{out}
Top	190	1.47×10^8	14,000	7.5	3.675	11.1	20,215	89,005	248,655	0.940
Bottom	250	1.47×10^8	—	—	0.504	4.40	14,848	77,626	238,706	0.567

section and a 54 m^3 bottom section. In order to model the reactor, each section was divided into 30 wall cells and 30 shaft cells. Ethylene, chain transfer agent (S) and peroxide are fed at cell 14 at the top section. Peroxide is fed at cell 6 at the bottom section. The main operating conditions are summarized in *Table 1*, together with some of the results from the moment model. The kinetic parameters used and other details may be found elsewhere (1).

We show in *Fig. 3* the calculated chromatographic pgf for the top and bottom sections of the reactor. There is little difference between the curves corresponding to the two zones. Similar curves are obtained for the number and weight pgf, where the observed difference is even smaller. However those differences are enough to account for variations in MWD. Moreover, as we show later, the inversion method is sensitive to such small differences. The ordering of the curves, with pgfn > pgfw > pgfc is always respected for the cases tried. Comparing *Figs. 2* and *3* evidences that the pgf curves calculated from mass balances for case PE-B have general shapes very similar to those calculated for other polymers starting from their experimental MWDs. This indicates that the model produces reasonable pgf functions.

The corresponding chromatographic distributions at the end of the top and bottom zones, calculated by inverting the above pgf, are shown in *Fig. 4*. They were obtained as previously suggested (3), using the optimum value of the parameter h or N, depending on the inversion method used, as indicated in the *Figure*. For the remaining MWDs, those same optimum values of N or h were used. The values of SSQ1 are all of the same order of magnitude (O (10^{-2})). It is worth to note that in these cases the number of evaluations of pgfs

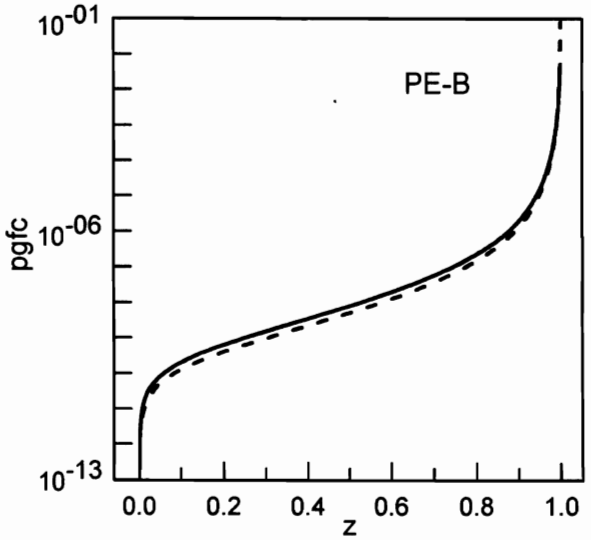

Fig. 3. Chromatographic probability generating functions obtained by the pgf model for PE-B at the top (- - -) and bottom zones (—).

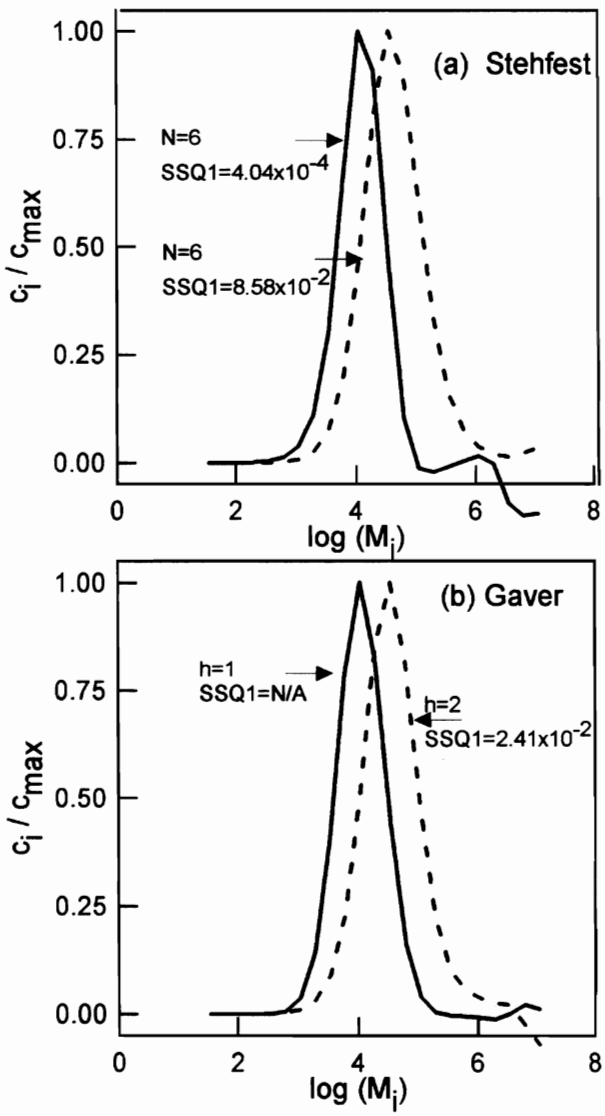

Fig. 4. Normalized chromatographic MWDs (c_i/c_{max}) at the top (- - -) and bottom zones (—), recovered from inversion of the corresponding pgf by (a) Stehfest's method, and (b) Gaver's method. Polymer: PE-B.

for each point of MWD recovered were $N_T = 8$ for Gaver's method and 6 for Stehfest's method. This indicates that one may obtain results of comparable quality using either inversion method, but Gaver's method is computationally more expensive. The values of N and h are similar to those reported in Brandolin *et al.* (3) as optimal for noisy pgfs. This suggests that the lower accuracy is due to the higher numerical error inherent in the pgf model resolution.

Qualitative results are the same using either method. Molecular weights are higher at the top zone, mainly because here the reactor operates at a lower temperature at which degradation reactions are negligible compared to propagation and termination by combination reactions. Moreover the kinetic constant for the first initiator decomposition is lower, giving more time for the molecules to grow. Molecular weight distributions by number and weight were predicted as unimodal, with no special features. In contrast, the chromatographic distributions (*Figs. 4a* and *b*), show an oscillation in the bottom zone around a molecular weight of 1×10^6 when using Stehfest's method, and near 1×10^7 when using Gaver's method. It would be difficult to decide whether this oscillation is due to a numerical problem or it reflects an actual shoulder in the curve if the SSQ1 criterion was not available. Nevertheless it must be remembered that the most reproducible prediction is that of weight MWD (3). This may be attributed to the fact that it does not stress the low molecular weights, as the number distribution does, nor the very high molecular weight tail, as the chromatographic distribution.

When applying the model to polymers obtained in the industrial reactor, average molecular weights were predicted with excellent accuracy for the selected polyethylenes (PE-1 and PE-2) and the copolymer EVA-17 by the moment model (1). In the case of EVA-7 an overprediction of number-average molecular weight was reported in our previous work. This overprediction could affect the subsequent results of the pgf model, so higher errors are expected for this copolymer.

Figures 5 to *7* present the three types of experimental MWDs together with the ones obtained through the inversion of the corresponding pgf for the studied polymers at the reactor exit. Those pgfs were calculated through the pgf model. In all cases, the optimum inversion parameters were N=6 for Stehfest's method and h=2 for Gaver's method with the exception of the number distribution at the reactor exit for PE-1, where N=8 is the optimum value. In all cases the order of magnitude of SSQ1 was of 5×10^{-2}. As indicated in the case of PE-B, Stehfest's method is computationally less expensive. Nevertheless the results obtained with both methods are of comparable quality.

From the physical and chemical point of view, we observed that distributions for PE-1 and PE-2 showed a shift towards lower molecular weights as the mixture flows from the top to the bottom zone. This behavior is similar to that observed for PE-B, as explained above. For EVA-7 and EVA-17 the shift is not clearly defined, probably because the temperature gap between top and bottom zones is lower than in the case of polyethylenes.

When comparing number MWD predictions with the measured data, agreement was qualitatively good (see *Fig. 5*). It must be kept in mind that the experimental data points were obtained through conversion of the measured chromatographic distribution. Since the SEC technique always gives better values of weight averages than number averages, errors are magnified for the short molecules. The least accurate predictions come out for the polyethylenes, especially for PE-1. In this case the measured chromatogram presented high level of noise in the lower molecular weight band (see *Fig. 6a*), making the converted number MWD unreliable. Predictions for EVA (*Figs. 5c* and *5d*) are much better, this may be attributed to their simpler MWD curves.

Figure 6 shows the comparison between experimental and calculated weight MWDs. The results were satisfactory for most of the polymers, as expected from the findings in the PE-B case that were discussed above. For EVA-7, a small overprediction was obtained at the high molecular weight region, as expected due to the differences between experimental average molecular weights and those obtained through the moment model. Gaver's method seems to lead to slightly better weight MWD predictions at the reactor exit.

The chromatographic distributions are presented in *Fig. 7*. It was found that all distributions could be predicted fairly well from pgfc. The best predictions for PE-1 and EVA-17 were obtained using Stehfest's inversion. The low molecular weight shoulder present in the PE-1 chromatographic MWD was overly amplified when using Gaver's inversion. In the case of PE-2 it was not possible to predict the shoulder present in the experimental curve for molecular weights higher than 1×10^6 using either method. This is probably due to numerical problems and error propagation in pgf inversion, which is worse at higher molecular weights. It would be possible to recover it if error propagation did not mask the results obtained with higher values of the h or N parameter (3). Another possibility is that the selected kinetic mechanism is not complete enough to describe the complete MWD, even though it allows good average molecular weight predictions. Finally, the shape and width of EVA-7 chromatographic distribution was satisfactorily predicted by both methods but the calculated MWD was shifted towards higher molecular weights. This is in accordance with the overprediction of average molecular weights by the moment model.

CONCLUSIONS

We have solved a system of transformed mass balance equations that describe the polymerization of ethylene or ethylene-vinyl acetate in industrial autoclave reactors. We have applied the pgf transform and have used three expressions for it, each one meant to best describe either the number, weight or chromatographic

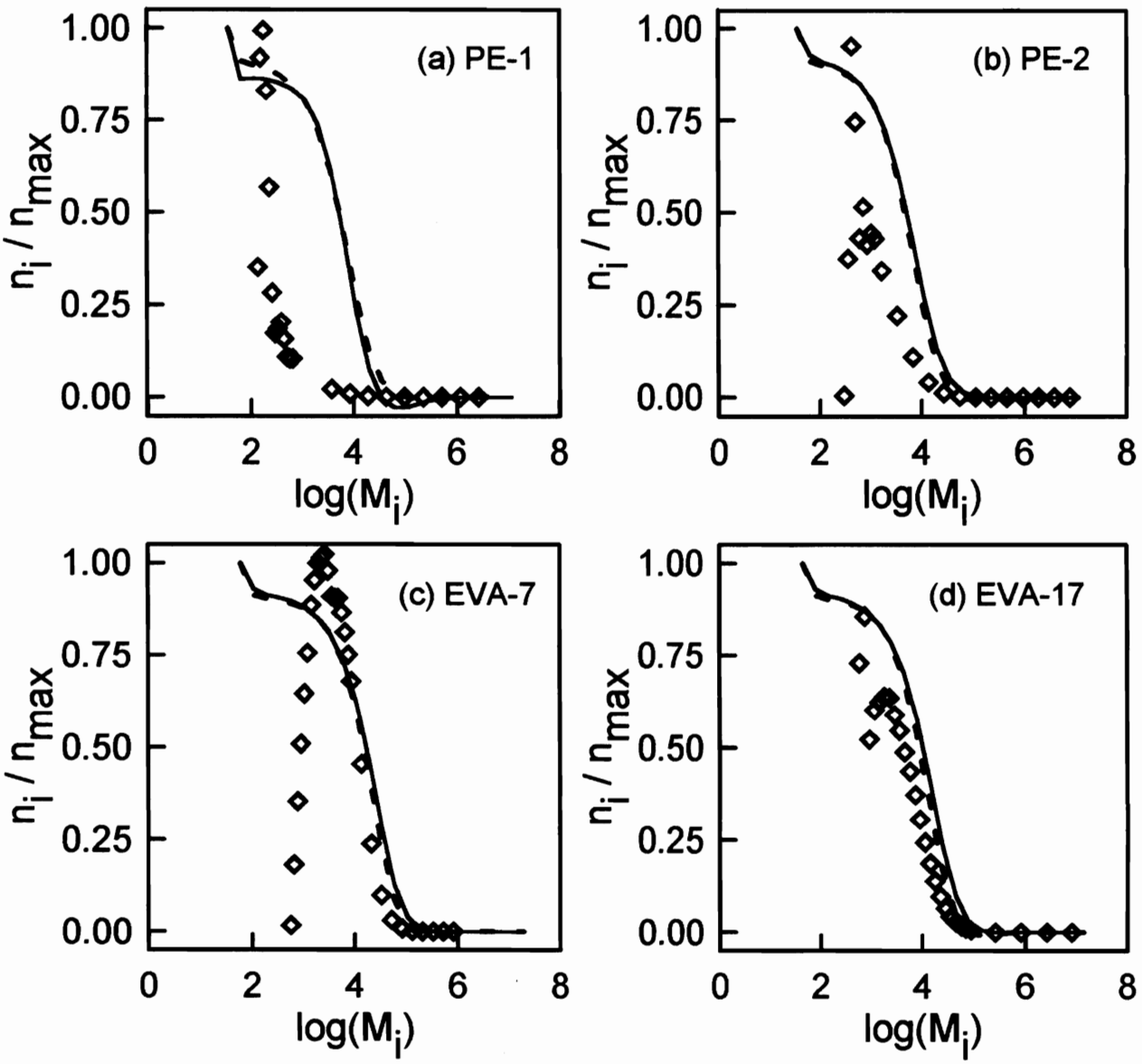

Fig. 5. Measured (◇) and calculated normalized number MWDs (n_i/n_{max}) at the bottom zone, recovered from inversion of the corresponding pgf by Stehfest's method (—), and Gaver's method (- - -). Polymers:PE-1, PE-2, EVA-7 and EVA-17.

MWD of the polymers produced in the reactors. Numerical inversion of the transformed variables has allowed a very good recovery of the entire molecular weight distribution, as compared with the experimental distributions measured by SEC. The inclusion of pgfw and pgfc definitions into the pgf model results in reliable predictions of weight and in particular of chromatographic distributions, attenuating the noise due to inversion typical of the high molecular weight tail.

The two numerical inversion methods used gave results of comparable quality, but Stehfest's inversion required less computational effort.

Overall, our model at its present stage of development constitutes a viable alternative to pilot plant or industrial scale trial-and-error experiments, with economic and safety advantages. It is a tool that has potential in optimization studies of industrial reactors and in the development of new polymer grades.

ACKNOWLEDGMENT

The Repsol-YPF authors would like to acknowledge the contribution of A. Gilchrist and R.A. Jackson of ICI in providing a simple stirring current model from which the more elaborate model was developed. We are indebted to M. Aroca (Repsol-YPF) for the molecular weight measurements. We also must mention A. Garriga and M. Asteasuain for their contribution to the numerical inversion. The PLAPIQUI authors would like to acknowledge CONICET for financial support. We thank Dr. P.E. Ugrin for his efforts in data collection.

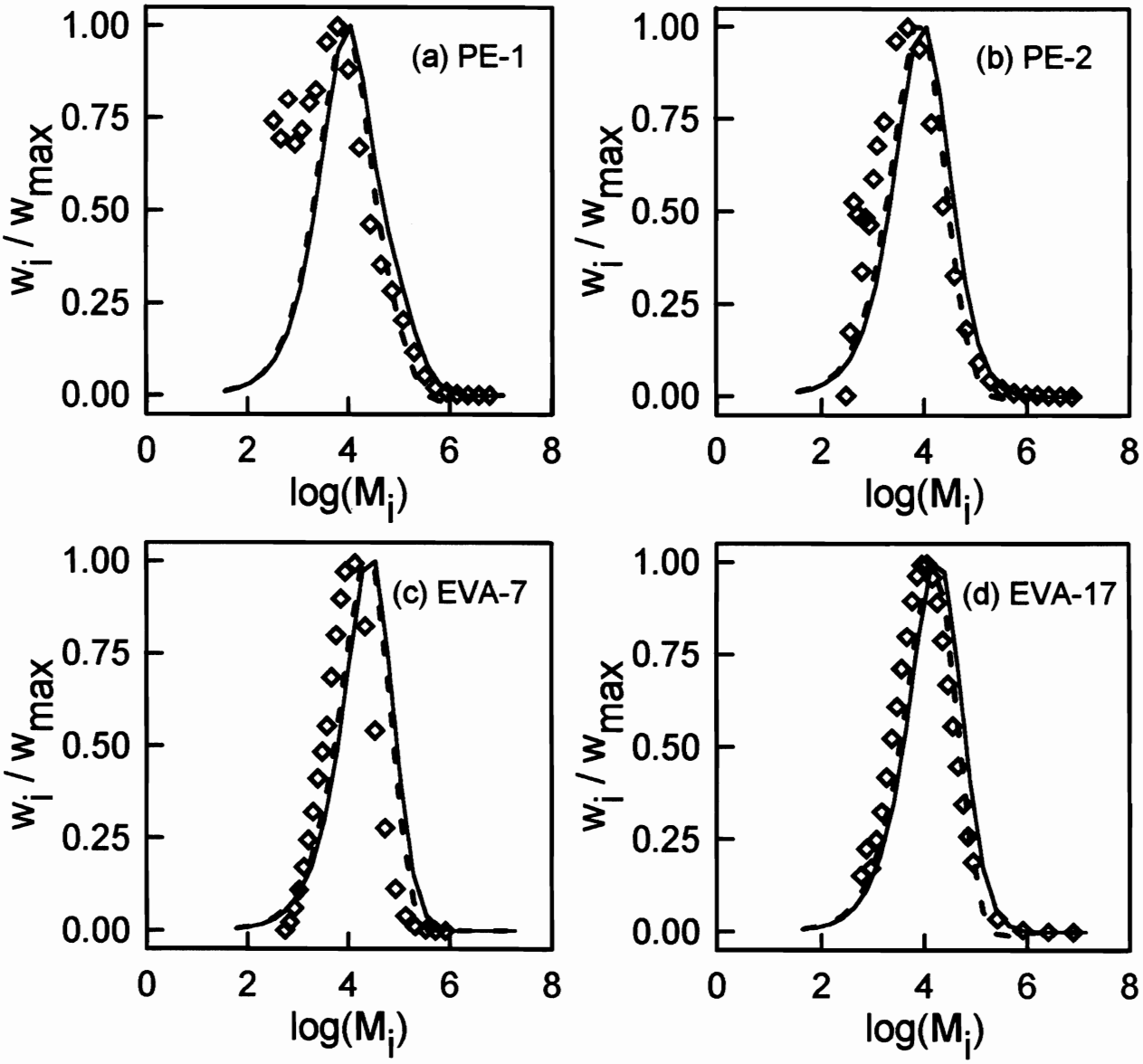

Fig. 6. Measured (◇) and calculated normalized weight MWDs (w_i/w_{max}) at the bottom zone, recovered from inversion of the corresponding pgf by Stehfest's method (—), and Gaver's method (- - -). Polymers:PE-1, PE-2, EVA-7 and EVA-17.

NOMENCLATURE

c_i = Chromatographic fraction of molecules in the ith fraction of the chromatogram
$Conv$ = Monomer conversion at reactor outlet
DP_i = Degree of polymerization in the ith fraction of the chromatogram, i = 1,2,...
f_j = Initiation efficiency of the "j" peroxide initiator, j = 1,2...
F_V = Generic volumetric flow
Fg = Mass flow rate of fresh monomer gas
h = Gaver's parameter
I_j = "j" peroxide initiator, j = 1,2,...
k_{ej} = Kinetic constant for "j" peroxide initiation, j = 1,2...
k_p = Kinetic constant for propagation reaction
k_{tc} = Kinetic constant for termination by combination reaction
k_{tdt} = Kinetic constant for termination by thermal degradation
k_{trm} = Kinetic constant for transfer to monomer reaction
k_{trp} = Kinetic constant for transfer to polymer reaction
k_{trsj} = Kinetic constant for transfer to "j" solvent reaction, j = 1,2...
Ln = Long chain branching index (/1000C)
M = Global monomer
$\bar{M}_{mon}$ = Monomer average molecular weight
Mn = Number-average molecular weight
Mw = Weight-average molecular weight
Mz = z-average molecular weight

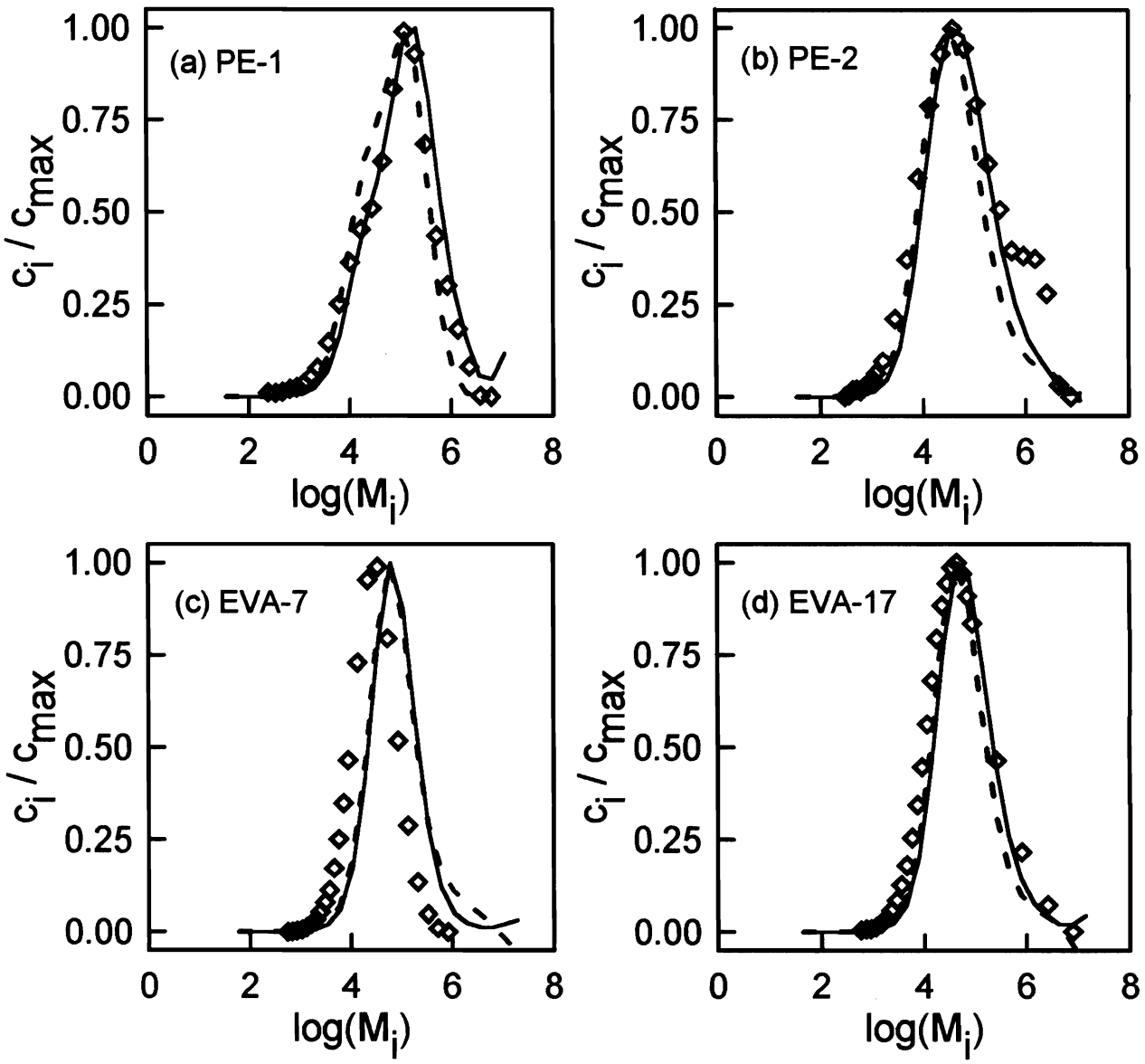

Fig. 7. Measured (◇) and calculated normalized chromatographic MWDs (c_i/c_{max}) at the bottom zone, recovered from inversion of the corresponding pgf by Stehfest's method (—), and Gaver's method (- - -). Polymers:PE-1, PE-2, EVA-7 and EVA-17.

N = Stehfest's parameter
N_{eq} = Number of equations to be solved at each section
n_i = Number fraction of molecules in the ith fraction of the chromatogram, i = 1,2...
N_T = Total number of pgf evaluations
N_w = Number of points of the MWD to be evaluated
Nz = Number of reactor zones
$Ncell$ = Total number of cells in which a section is divided
Nin = Number of entrances to a cell
NIT = Total number of peroxide initiators
$Nout$ = Number of exits from a cell
NST = Total number of solvents
P = Operating pressure
$P(x)$ = Polymer with "x" monomer units, x = 1...∞
$P_j(X = x)$ = Number (j=n), weight (j=w) or chromatographic probability (j=c) of radicals having a degree of polymerization equal to "x"
$P_j^*(X = x)$ = Number (j=n), weight (j=w) or chromatographic probability (j=c) of polymer having a degree of polymerization equal to "x"
$R(0)$ = Radical without monomer, produced by peroxide decomposition

$R(x)$ = Radical with "x" monomer units, x = 0...∞
S_j = "j" solvent, j = 1,2...
T_{set} = Temperature of set
V = Volume
VA = Vinyl-Acetate
w_i = Weight fraction of molecules in the ith fraction of the chromatogram, i = 1,2...
z = Transformed variable in pgf functions

Greek Symbols

δ_{ij} = Kronecker's Delta
λ_n = nth moment of the size distribution of radicals
μ_n = nth moment of the size distribution of polymer
$\phi_{X,j}(z)$ = Number (j=n), weight(j=w) or chromatographic (j=c) probability generating function for size distribution of radicals
$\psi_{X,j}(z)$ = Number (j=n), weight(j=w) or chromatographic (j=c) probability generating function for size distribution of polymer

Subscripts and Superscripts

$'$ = Derivative
in = Input
I = Input/output counter
k = Generic cell counter
ks = Shaft cell counter
kw = Wall cell counter
out = Output

REFERENCES

1. C. Sarmoria, A. Brandolin, A. López-Rodríguez, K. S. Whiteley, and B. del Amo Fernández, *Polym. Eng. Sci.*, **40**, 1480 (2000).
2. A. López-Rodríguez, J. J. Pedraza, and B. del Amo, *Computers Chem. Eng.*, **20**, S1625 (1996).
3. A. Brandolin, M. Asteasuain, C. Sarmoria, A. López-Rodríguez, K. S. Whiteley, and B. del Amo Fernández, *Polym. Eng. Sci.*, in press.
4. R. A. Jackson, P. A. Small, and K. S. Whiteley, *J. Polym. Sci. Polym. Chem. Ed.*, **11**, 1781 (1973).
5. N. C. Miller, R. W. Toffolo, K. B. McAuley, and P. J. McLellan, *Polym. Reac. Eng.*, **4**, 279 (1996).
6. P. Lorenzini, M. Pons, and J. Villermaux, *Chem. Eng. Sci.*, **47**, 3969 (1992).
7. A. Brandolin, M. H. Lacunza, P. E. Ugrin, and N. J. Capiati, *Polym. Reac. Eng.*, **4**, 193 (1996).
8. H. Nordhus, Ø. Moen, and P. Singstad, *J. Macromol. Sci., Pure Appl. Chem.*, **A34**, 1017 (1997).
9. P. Pladis and C. Kiparissides, *Chem. Eng. Sci.*, **53**, 3315 (1998).
10. K. S. Whiteley and A. Garriga, *Comput. Theor. Polym. Sci.*, **11**, 319 (2001).
11. D. R. Miller and C. W. Macosko, *J. Polym. Sci. B*, **26**, 1 (1988).
12. W. Feller, *An Introduction to Probability Theory and Its Applications*, 3rd Ed., Vol. 1, Chap. 11, John Wiley & Sons, New York (1968).
13. M. J. D. Powell, *A Hybrid Method for Non-Linear Equations, in Numerical Methods for Non-Linear Algebraic Equations*, P. Rabinowitz, ed., Gordon and Breach, London (1970).
14. D. P. Gaver, Jr., *Oper. Res.*, **14**, 444 (1966).
15. H. Stehfest, *Comm. ACM*, **13**, 47 (1970).
16. H. Stehfest, *Comm. ACM*, **13**, 624 (1970).